

DOMAIN-AWARE TENSOR NETWORK STRUCTURE SEARCH

Giorgos Iacovides^{1*}, Wuyang Zhou^{1*}, Chao Li², Qibin Zhao², Danilo Mandic¹

¹Department of Electrical and Electronic Engineering, Imperial College London ²RIKEN AIP

{giorgos.iacovides20, wuyang.zhou19, d.mandic}@imperial.ac.uk

{chao.li, qibin.zhao}@riken.jp

ABSTRACT

Tensor networks (TNs) provide efficient representations of high-dimensional data, yet identification of the optimal TN structures, the so called tensor network structure search (TN-SS) problem, remains a challenge. Current state-of-the-art (SOTA) algorithms solve TN-SS as a purely numerical optimization problem and require extensive function evaluations, which is prohibitive for real-world applications. In addition, existing methods ignore the valuable domain information inherent in real-world tensor data and lack transparency in their identified TN structures. To this end, we propose a novel TN-SS framework, termed the tnLLM, which incorporates domain information about the data and harnesses the reasoning capabilities of large language models (LLMs) to *directly* predict suitable TN structures. The proposed framework involves a domain-aware prompting pipeline which instructs the LLM to infer suitable TN structures based on the real-world relationships between tensor modes. In this way, our approach is capable of not only iteratively optimizing the objective function, but also generating domain-aware explanations for the identified structures. Experimental results demonstrate that tnLLM achieves comparable TN-SS objective function values with much fewer function evaluations compared to SOTA algorithms. Furthermore, we demonstrate that the LLM-enabled domain information can be used to find good initializations in the search space for sampling-based SOTA methods to accelerate their convergence while preserving theoretical performance guarantees.

1 INTRODUCTION

The exponential increase in the volume and richness of available data has led to the widespread use of multi-way arrays, often represented as higher-order tensors. Tensor network decomposition methods aim to represent higher-order tensors in “super-compressed” formats through smaller-sized components, by effectively capturing cross-modal latent patterns and correlations. These methods have been applied across various fields, including machine learning (Zhe et al., 2015; Cichocki et al., 2016; Malik, 2021), signal processing (Zheng et al., 2023), computer vision (Shakeri & Zhang, 2019; Yamamoto et al., 2022), and quantum physics (Orús, 2019; Felser et al., 2021). The success of tensor network decomposition techniques is closely linked to their ability to mitigate the “curse of dimensionality”, which is achieved by decomposing higher-order data into lower-order factors.

However, tensor network (TN) practitioners face significant challenges related to choosing the most appropriate TN structure, the so called *tensor network structure search (TN-SS)* problem, which has been proven to be NP-hard (Hillar & Lim, 2013; Li et al., 2023). TN-SS involves determining the optimal TN parameters, such as TN ranks, TN topology, and TN mode permutations (Li et al., 2022).

Existing TN-SS methods solve TN-SS as a purely numerical optimization problem and include approaches such as Bayesian inference (Zeng et al., 2024b), spectrum methods (Chen et al., 2024), reinforcement learning (Meirom et al., 2022), discrete optimization (Li et al., 2022; 2023), and continuous optimization (Zheng et al., 2024). To date, sampling-based methods (Li & Sun, 2020; Li et al., 2022; 2023; Zeng et al., 2024a), whose workflows are illustrated in Figure 1a and 1b, have demonstrated the best performance in addressing the TN-SS problem.

*Equal Contribution

However, these methods require large number of evaluations (of the training and testing data), are prone to getting stuck in local minima, and lack transparency in their found structure-related parameters (Li et al., 2023). Critically, a large number of evaluations needed to optimize the objective function leads to a high computational cost. We hypothesize that these limitations arise from failing to exploit the rich domain information inherent in real-world tensors, such as the mode information. To this end, we ask ourselves:

How can we utilize the intrinsic domain information in tensor data to significantly reduce the number of evaluations required to solve the TN-SS problem, while providing domain-aware explanations for the identified TN solutions?

To address this question, we propose a domain-aware large language model (LLM)-guided TN-SS framework, termed tnLLM. Within this framework, an LLM is utilized to initialize the TN structure based on domain information about the relationships between tensor modes. Then, the reasoning capabilities of the LLM are used to navigate the search space effectively, in order to achieve good optimization of the objective function with very few evaluations.

Our proposed framework is found to achieve significant speed-ups over current state-of-the-art (SOTA) methods in terms of the number of evaluations, due to its ability to find good TN structure initializations through the use of domain information. Moreover, tnLLM generates practically meaningful explanations for the TN solutions, thus offering transparency in the identified structures. This is particularly beneficial for tensor practitioners who lack deep expertise in a specific data domain, as it enables them to both comprehend the interactions between tensor modes and trust the discovered TN structures. It also allows the identified structures to be verified by domain experts.

To evaluate the effectiveness of tnLLM, we compare its performance against SOTA TN-SS algorithms on real-world tensor datasets of order-3, 4, and 5. The experimental results demonstrate that tnLLM delivers performance comparable to current SOTA methods, while requiring significantly fewer function evaluations and providing domain-aware explanations for the identified TN structures. Moreover, we constructed a hybrid algorithm to combine the speed-up benefits of tnLLM with the theoretical guarantees of existing sampling-based approaches. The main contributions of this work are:

- We propose tnLLM, a novel domain-aware LLM-guided TN-SS framework, which achieves performance on par with SOTA methods while requiring much fewer evaluations;
- To the best of our knowledge, our framework is the first to utilize domain information inherent in real-world tensor data to address the TN-SS problem. This enables the generation of domain-aware explanations that allows practitioners to verify the identified TN structures.

1.1 RELATED WORK

Tensor network structure search (TN-SS). Compared to traditional tensor decompositions (Hitchcock, 1927; Tucker, 1966; Oseledets, 2011; Zhao et al., 2016; Wu et al., 2022), which have pre-defined tensor network structures, the TN-SS problem focuses on finding custom tensor networks, which have been shown to achieve higher parameter efficiency and are an important paradigm of tensor decompositions (Li et al., 2022; 2023; Li & Sun, 2020; Zeng et al., 2024a). Various approaches have been proposed to address the TN-SS problem, including Bayesian inference (Zeng et al., 2024b), spectrum methods (Chen et al., 2024), reinforcement learning (Meirom et al., 2022), program synthesis (Guo

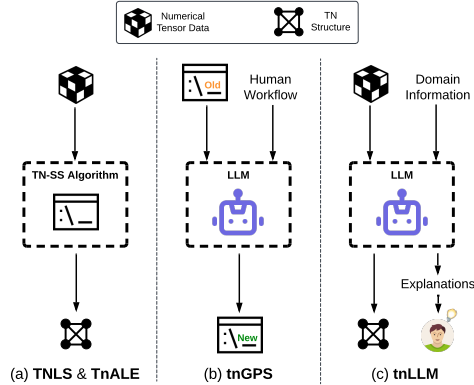


Figure 1: Comparison of SOTA tensor network structure search (TN-SS) methods. (a) TN-SS algorithms with theoretical guarantees: TNLS (Li et al., 2022) & TnALE (Li et al., 2023). (b) tnGPS (Zeng et al., 2024a), a prompting pipeline which uses LLMs to generate new TN-SS algorithms. (c) tnLLM (ours), which uses domain information about the tensor data and LLM reasoning to solve the TN-SS problem and generate explanations for the identified TN structure.

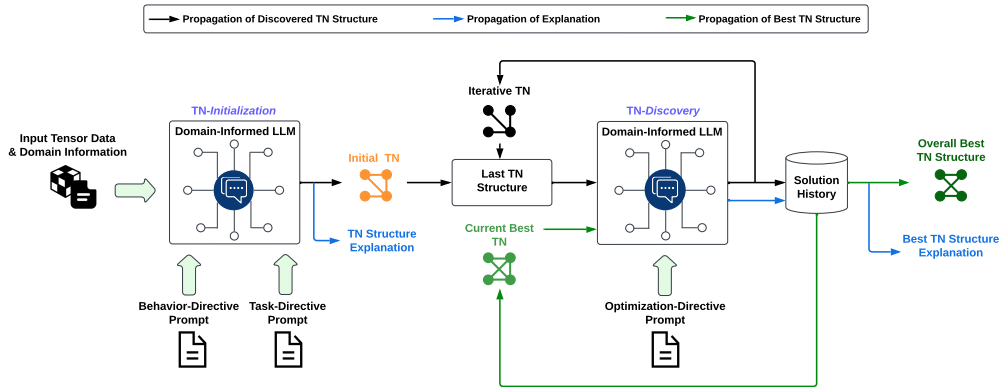


Figure 2: The workflow of the proposed tnLLM framework consists of two key stages commonly adopted by SOTA TN-SS methods (Li et al., 2022; 2023; Zeng et al., 2024a): *TN-initialization* and *TN-discovery*. The proposed tnLLM efficiently utilises the domain information in tensor data and uses an LLM to guide these two stages.

et al., 2025), and continuous optimization (Zheng et al., 2024). Sampling-based methods (Li et al., 2023; 2022; Li & Sun, 2020; Zeng et al., 2024a), which fall under discrete optimization methods, have demonstrated superior performance compared to other approaches in addressing the TN-SS problem. Among these, TNLS (Li et al., 2022) and TnALE (Li et al., 2023) achieve state-of-the-art (SOTA) performance, with TnALE accelerating TNLS by slightly reducing the number of evaluations required to optimize the objective function. While both TNLS and TnALE adopt a “local-search” scheme, this acceleration is achieved by the alternating variable updates proposed in TnALE. However, these methods still face challenges, such as a large number of function evaluations required to converge, difficulty in balancing exploration and exploitation, and a lack of transparency in the found structures.

More recently, tnGPS (Zeng et al., 2024a) has emerged as an approach that uses LLMs to generate sampling-based TN-SS algorithms, demonstrating performance comparable to SOTA methods. Despite being closest to our work, tnGPS focuses on generating TN-SS algorithms based on sampling-based heuristics and does not incorporate any domain information in the tensor data. As such, tnGPS suffers from the same limitations as existing sampling-based methods, including a lack of explainability in the identified structure-related parameters.

To this end, our work proposes to harness the domain information in tensor data to solve the TN-SS problem. We achieve this by using the domain knowledge and the inherent reasoning capabilities of LLMs to *directly* infer tensor network structures. Facilitated by our carefully designed prompting pipeline (see Section 3), the proposed framework is shown not only to require significantly fewer evaluations, but also to produce domain-aware and verifiable solutions to the TN-SS problem.

Reasoning with large language models. The rise of transformer-based LLMs, pretrained on vast text corpora, has demonstrated a remarkable capacity for “reasoning” (Wei et al., 2022a). This reasoning ability is further enhanced when LLMs are guided by task-specific prompting strategies, such as chain-of-thought (Wei et al., 2022b; Suzgun et al., 2023; Kojima et al., 2024). These strategies enable LLMs to generate text effectively for tasks such as arithmetic reasoning and factual knowledge retrieval, leading to exceptional performance in complex question-answering and tasks requiring real-world knowledge (Liévin et al., 2023; Singhal et al., 2023). These findings suggest that, through pretraining on diverse textual data, LLMs encode rich knowledge about real-world relationships, which they can effectively leverage to perform various downstream tasks (Choi et al., 2022). In this work, we utilize the real-world domain knowledge and “reasoning” capabilities of LLMs to directly infer suitable TN structures.

Algorithm 1: Sampling-based Algorithms for TN-SS (Li et al., 2022; 2023; Zeng et al., 2024a)

```

1: Initialize:
2:  $N_{Iter}$  ▷ Maximum number of iterations
3:  $N_{Sample}$  ▷ Number of samples per iteration
4:  $P \leftarrow \emptyset$  ▷ Historical TN structures
5:  $H \leftarrow \emptyset$  ▷ Discovered TN structures in each iter.
6:  $\mathcal{F}(\cdot) \leftarrow$  Equation (1) ▷ Objective function
7:  $(G, \mathbf{r}) =$  Initial TN Structure ▷ TN-initialization
8:
9: Algorithm:
10: for  $n = 1$  to  $N_{Iter}$  do
11:    $H \leftarrow N_{Sample}$  TN structures sampled in the neighborhood of  $(G, \mathbf{r})$ . ▷ TN-discovery
12:    $P \leftarrow P \cup H$ 
13:   if  $\exists (\hat{G}, \hat{\mathbf{r}}) \in P$  such that  $\mathcal{F}(\hat{G}, \hat{\mathbf{r}}) < \mathcal{F}(G, \mathbf{r})$  then
14:      $(G, \mathbf{r}) \leftarrow (\hat{G}, \hat{\mathbf{r}})$ .
15:   if Converged then
16:     return  $(G, \mathbf{r})$ 
17: Output:  $(G, \mathbf{r})$ 

```

2 PRELIMINARIES

2.1 TENSOR NETWORK STRUCTURE SEARCH (TN-SS)

We first provide the definition of TN-SS through its application in higher-order data decomposition. An optimal solution to the TN-SS problem aims to find the best trade-off between identifying the most compressed TN structure while preserving the expressivity of the TN (Li & Zhao, 2021). Let $\mathcal{X} \in \mathbb{R}^{I_1 \times I_2 \times \dots \times I_N}$ be a non-zero order- N tensor, with its Frobenius norm as $\|\mathcal{X}\|_F$. Tensor networks can be represented using the graphical notation (Orús, 2014; Ye & Lim, 2018), whereby a tensor network G is represented using a set of N vertices, V , and a set of edges, E , i.e., $G = (V, E)$. Each vertex represents a decomposed core tensor, and the closed edges between two core tensors are generalized higher-order matrix multiplications, termed tensor contractions (Cichocki et al., 2016). Closed edges have assigned *TN-ranks*, $\mathbf{r} \in \mathbb{Z}_+^E$, which indicate the degree of connectivity between different pairs of connected vertices. Therefore, the properties of a TN structure can be fully expressed by the combination (G, \mathbf{r}) .

Similar to SOTA TN-SS methods (Li & Sun, 2020; Li et al., 2023; 2022; Zeng et al., 2024a), the discrete optimization problem of TN-SS is formalized as a minimization of the objective function, which is a linear sum of the complexity of the TN structure (e.g., compression rate) and the TN expressivity (e.g., approximation error), and is given by

$$\min_{(G, \mathbf{r})} \ln \left(\phi(G, \mathbf{r}) + \frac{\lambda}{L} \min_{\{\mathcal{V}_{l,i}\}_{i=1}^N} \sum_{l=1}^L \frac{\|\mathcal{X}_l - TNC(\{\mathcal{V}_{l,i}\}_{i=1}^N; (G, \mathbf{r}))\|_F}{\|\mathcal{X}_l\|_F} \right) \quad (1)$$

where L represents the number of tensor samples in the dataset, and the first term $\phi(G, \mathbf{r})$ measures the TN structure complexity. The second term in Equation (1) measures the expressivity of the TN through the relative squared error (RSE) between the original tensors $\{\mathcal{X}_l\}_{l=1}^L$ and their TN approximations $\{TNC(\{\mathcal{V}_{l,i}\}_{i=1}^N; (G, \mathbf{r}))\}_{l=1}^L$, where $TNC(\cdot)$ stands for the tensor contraction operation of the entire tensor network. The pair (G, \mathbf{r}) characterizes how the vertices, $\{\mathcal{V}_{l,i}\}_{i=1}^N$, are contracted together to approximate the original tensor \mathcal{X}_l . The coefficient λ is a positive non-zero scaling factor which balances the trade-off between model complexity and model expressivity. Note that (Li & Sun, 2020; Ye & Lim, 2018) pointed out that the TN-SS problem is conveniently equivalent to the TN rank search problem of a fully connected TN (Zheng et al., 2021).

2.2 SOTA SAMPLING-BASED ALGORITHMS FOR TN-SS

Algorithm 1 summarizes the current SOTA algorithms for TN-SS. They follow a three-step search process: *TN-initialization* \rightarrow *TN-discovery* via sampling in the search neighborhood \rightarrow Updating the center of the search neighborhood. Existing methods ignore the inherent domain information in

real-world tensor data, which calls for the development of a framework that can effectively utilize domain knowledge in *TN-initialization* and *TN-discovery* to improve performance.

To this end, our proposed framework introduces domain-aware LLM-guided *TN-initialization* and *TN-discovery*. By doing so, it addresses the limitations of existing methods, such as high computational costs caused by the large number of evaluations ($N_{Iter} \times N_{Sample}$) required and the tendency to get stuck in local minima due to difficulties in balancing the exploration-exploitation trade-off. Importantly, by incorporating domain information, our tnLLM framework provides practically meaningful explanations for the identified TN structures, a feature absent in current approaches.

3 TNLLM: A DOMAIN-AWARE FRAMEWORK FOR SOLVING TN-SS

This section presents tnLLM, a domain-aware LLM-guided framework that efficiently solves the TN-SS problem with very few evaluations and verifiable solution explanations. We detail the role of each component in the prompting pipeline and the guidelines followed by each prompt.

Workflow of tnLLM. Figure 2 illustrates the workflow of the proposed tnLLM framework. The “Behavior-directive” prompt is used to supply the problem specification and guide the general-purpose LLM into a model tailored for solving the TN-SS problem. Inspired by current sampling-based SOTA algorithms, this domain-informed LLM is then employed for LLM-guided *TN-initialization* and *TN-exploration*.

During the *TN-initialization* stage, the “Task-directive” prompt is used to propose a strong initial TN structure by using the provided domain information. In the *TN-discovery* stage, the last and best-identified TN structures are used in conjunction with the “Optimization-directive” prompt to guide the LLM in navigating the search space effectively. The identified TN structures are fed into an objective function evaluation program to obtain the objective function values. This iterative process leads to the refinement of the TN structure and yields improved objective function values over successive evaluations.

Prompting pipeline. The interactions between the carefully designed user prompts and the LLM assistant follow an automated structured dialogue (OpenAI, 2023; Touvron et al., 2023). This dialogue-based approach is intuitive for generating stepwise conversational reasoning and is particularly useful for iterative tasks such as the TN-SS problem. To further improve the ability of the LLM to perform complex reasoning, we employ the chain-of-thought prompting (Wei et al., 2022b). This prompting strategy breaks down complex tasks into a series of intermediate reasoning steps and thus enables the model to solve the problem by addressing smaller, simpler sub-tasks sequentially. In the proposed tnLLM framework, three distinctly purposed prompts are employed, each serving a unique role. The full prompts are given in Appendix B.

“Behavior-directive” prompt. This is the system message in the dialogue. Its primary objective is to establish the role of the LLM as an expert in the TN-SS problem (orange section of Figure 3a) and guide its behavior throughout the dialogue (green section of Figure 3a). Additionally, it sets the context by outlining the TN-SS problem and the objective function (blue section of Figure 3a).

“Task-directive” prompt. This is the first non-system prompt supplied to the LLM and serves as the basis for LLM-guided *TN-initialization*. It is designed to thoroughly explain the domain information about the tensor structure, including details such as the number of modes and the specific information about each mode (orange section of Figure 3b). Furthermore, it guides the model’s thought process and ensures that its responses align with the task requirements by instructing it to reason step-by-step and utilize domain knowledge (blue section of Figure 3b).

“Optimization-directive” prompt. This is the iterative prompt supplied to the LLM in all subsequent evaluations and serves as the basis for LLM-guided *TN-discovery*. Its purpose is to guide the LLM to efficiently navigate the search space by incorporating context from the best and previous evaluations (orange section of Figure 4). The prompt explains how refinements to the identified TN structure influence the objective function value and instructs the model to leverage step-by-step reasoning and domain knowledge to optimize the objective function (blue section of Figure 4). At the



Figure 3: Structure and components of (a) the “Behavior-directive” prompt, which frames the LLM’s role as a domain expert, and (b) the “Task-directive” prompt for LLM-guided *TN-initialization*.

same time, it encourages the LLM to both *explore* and *exploit* new solutions to reduce the likelihood of the method being stuck in local minima (purple section of Figure 4).

Efficient and effective search space navigation. A critical factor in the performance of tnLLM, both in terms of evaluations and objective function value, is the incorporation of memory (orange section of Figure 4) and the encouragement of search space "exploration and exploitation" (purple section of Figure 4) in the “Optimization-directive” prompt. By including the best and most recent TN solutions, along with their respective objective function values and the domain information about mode interactions, the LLM gains a better understanding of the search space and can make more informed decisions. Additionally, by encouraging the model to explore new solutions when necessary and exploit good solutions already found assists the optimization process, by reducing the possibility of the model getting stuck in local minima, a common caveat of sampling-based methods.

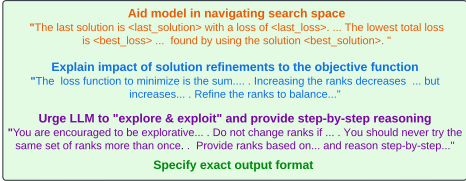


Figure 4: Structure and components of the “Optimization-directive” prompt used for LLM-guided *TN-discovery*.

Output format specification. As observed in Figures 3b and 4, in addition to the goal-oriented components of each prompt, an essential feature (highlighted in green) of both the “Task-directive” and “Optimization-directive” prompts is the specification of the exact output format of the TN-SS solution. This includes defining both the sequence in which the LLM should present its response and the precise format of the TN-SS solution. To meet these requirements, the prompt shown in Figure 5 was developed through experimentation and a trial-and-error process with the LLM. This step serves to eliminate “hallucinations” in the LLM output and enables a *fully automated* prompting pipeline without the need for any human intervention during the entire iterative optimization process.

Remark 3.1. Both tnGPS and tnLLM use LLMs to solve the TN-SS problem, however, the two approaches are fundamentally different. tnGPS uses the LLM to generate new *sampling-based TN-SS algorithms* by reviewing existing algorithms, causing the discovered methods to inherit similar limitations. In contrast, tnLLM uses the LLM to *directly infer TN structures* to solve the TN-SS problem by incorporating the rich domain information in real-world tensor data. In turn, this allows tnLLM to provide explanations for the TN solutions, thereby adding transparency to the identified TN structures.

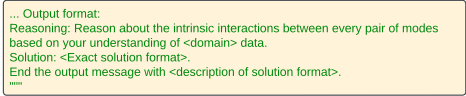


Figure 5: The prompt used to specify the LLM output format.

4 EXPERIMENTAL RESULTS

In this section, the performance of tnLLM was evaluated against the SOTA sampling-based methods in tensor decomposition tasks in terms of the number of evaluations and objective function value. Our results demonstrate that tnLLM achieves comparable objective function values while delivering significant speed-ups. Moreover, we demonstrate its ability to generate domain-consistent explanations

Table 1: Performance comparison across different datasets. The values on the left give the lowest training and corresponding testing objective function values. The values in [square brackets] give the number of evaluations required to first achieve the best training objective function value. For robustness assessment of tnLLM, we report the average and standard deviation of both the objective function value and the number of evaluations across 5 independent runs. For both metrics, a lower value is better. The best values are denoted in bold. The second best values are underlined.

Data Type		TNLS		TnALE		tnGPS		tnLLM (Ours)	
Images	Train	-0.66	[114]	-0.65	[81]	-0.66	[438]	-0.63±0.01	[4.0±1.9]
	Test	<u>-0.47</u>		-0.46		-0.44		-0.48±0.05	
Videos	Train	-1.64	[484]	-1.66	[254]	-1.65	[175]	-1.63±0.01	[6.2±3.5]
	Test	-1.72		-1.72		<u>-1.71</u>		-1.70±0.02	
Time-series	Train	-0.45	[218]	-0.47	[177]	-0.39	[38]	-0.42±0.02	[5.6±4.4]
	Test	<u>-0.43</u>		-0.47		-0.40		-0.41±0.02	

for the identified TN structures. Finally, an ablation study was conducted to evaluate the effectiveness of domain information and assess the framework’s robustness across different LLMs.

Data preparation. Given the flexibility of our method to handle tensor data of any order, we evaluated its performance on three types of tensor data with varying sizes and dimensionalities across different domains. In particular, we tested on datasets of order-3 RGB images and order-4 RGB videos. We also curated a completely new order-5 financial time-series dataset of 142 tensors to ensure that it was not included in the training data of LLMs. This time-series tensor dataset, to the best of our knowledge, is the largest dataset in terms of number of samples ever considered in the TN-SS problem. All entries were standardized to values in $[0, 1]$, with 80% of each dataset used for training, and the remaining 20% for testing. More details about the data can be found in Appendix C.

Settings of tnLLM. In Equation (1), we set $\lambda = 10$ and used the same compression ratio function, ϕ , as in previous sampling-based methods (Li & Sun, 2020), defined as the ratio between the number of parameters in the compressed TN format and the original tensor. The maximum number of evaluations was set to 500 for the images and videos datasets, and 250 for the financial time-series dataset. An early stopping criterion with a patience of 5 was applied. For all experiments, the LLM model GPT-4o (gpt-4o-2024-08-06) (OpenAI, 2024) was used, with temperature set at 0.2.

Implementation details. In all experiments, we also implemented the three SOTA sampling-based TN-SS algorithms, namely TNLS (Li et al., 2022), TnALE (Li et al., 2023) and tnGPS (Zeng et al., 2024a), and accelerated them with GPUs. Since the vanilla TNLS is designed to search only for the permutation of a TN, we extended it to fit the settings of TN-SS. For fair comparisons, all baseline methods were evaluated using the same objective function and maximum number of evaluations, with one evaluation defined as a single pass through the entire training and testing dataset. The full implementation details are provided in Appendix D.

Numerical results. We ran tnLLM five times and examined the mean and standard deviation for both the objective function values and the number of evaluations to demonstrate its *robustness*. Observe from Table 1 that tnLLM achieved performance on par with SOTA sampling-based algorithms in both training and test objectives across all data types, as measured by the objective function. Importantly, tnLLM minimizes the objective function with significantly fewer evaluations, requiring up to $78\times$ fewer evaluations than TNLS, $41\times$ fewer than TnALE, and $110\times$ fewer than tnGPS. Consequently, tnLLM achieves runtime reductions of up to 98.3% compared to TNLS, 97.7% compared to TnALE, and 98.1% compared to tnGPS, even after accounting for LLM inference. The full runtime comparisons are provided in Appendix E.

Domain-aware explanations. To assess the domain-relevance of the identified TNs, we manually verified the explanations provided for the identified TN structures in all three datasets tested. The explanations of the tnLLM model for the initialized TN structure, with and without domain knowledge, are provided in Figure 6. Observe that without domain information, although the model is inherently capable of reasoning, its lack of domain information about the modes in the real-world tensors causes

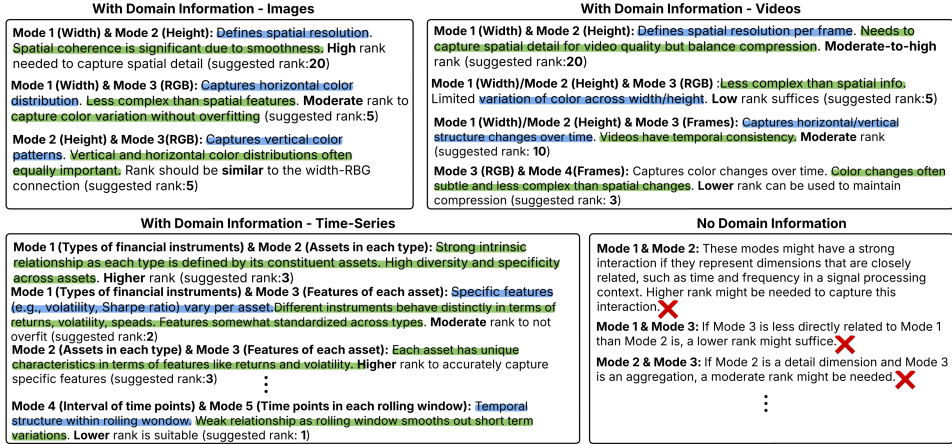


Figure 6: Summarized generated explanations of tnLLM for the initialized TN structure, with and without the incorporation of domain information in the prompts.

it to default to random assumptions, likely influenced by its pre-training data, such as assuming a mode as resembling time or frequency. As a result, the explanations are entirely incorrect from a practical perspective and are therefore ineffective in solving TN-SS.

In contrast, incorporating domain information enables the model to identify relationships between modes (highlighted in blue) and, more importantly, relate them to real-world principles in vision and finance (highlighted in green). The model also shows consistent reasoning in its rank suggestions: when describing a rank as low, medium, or high, it quantitatively selects a value that is coherent relative to other ranks within the same tensor. Moreover, it adjusts these values based on comparisons across different mode pairs, for example by assigning similar ranks to the Height–RGB and Width–RGB modes in the images dataset, and a lower rank to the RGB–Frames mode in the videos dataset. This demonstrates the model’s understanding of tensor mode relationships based on domain information and supports the validity of the identified TN structure. Consequently, tnLLM offers explanations that are practically useful in helping domain experts to verify and trust the discovered structures. Summarized explanations across three runs for all datasets are provided in Appendix F.

4.1 ACCELERATING SOTA METHODS WITH TNLLM

In the first part of Section 4, we have demonstrated that tnLLM achieves comparable objective function values compared to SOTA sampling-based algorithms, while generating domain-aware explanations for the identified TN structures and significantly reducing the required number of function evaluations. However, due to the black-box nature of LLMs, no theoretical analysis can be provided for the evaluation efficiency of tnLLM, in contrast to TNLS and TnALE.

At the same time, while sampling-based methods follow a “local-search” scheme within a neighborhood, there is no guarantee on the minimum number of evaluations required to find a “good” neighborhood. Moreover, poor initialization significantly increases the number of evaluations needed. To address this, we construct a hybrid algorithm that first runs tnLLM for 10 evaluations to leverage its domain knowledge and reasoning capabilities in order to identify a strong initialization point in the “global-search” stage. Sampling-based methods then perform “local-search” in the identified neighborhood, combining the speed-up benefits of tnLLM with their theoretical guarantees.

Numerical results. Figure 7 demonstrates the performance difference of TNLS and TnALE with and without a tnLLM-initialized structure. The “global-search” capability of tnLLM significantly sped up the iterative minimization process. During “local-search”, both TNLS and TnALE further improved upon the structures found in “global-search” by tnLLM. Overall, the tnLLM-initialized algorithms achieved nearly identical objective function values with up to 23× fewer evaluations

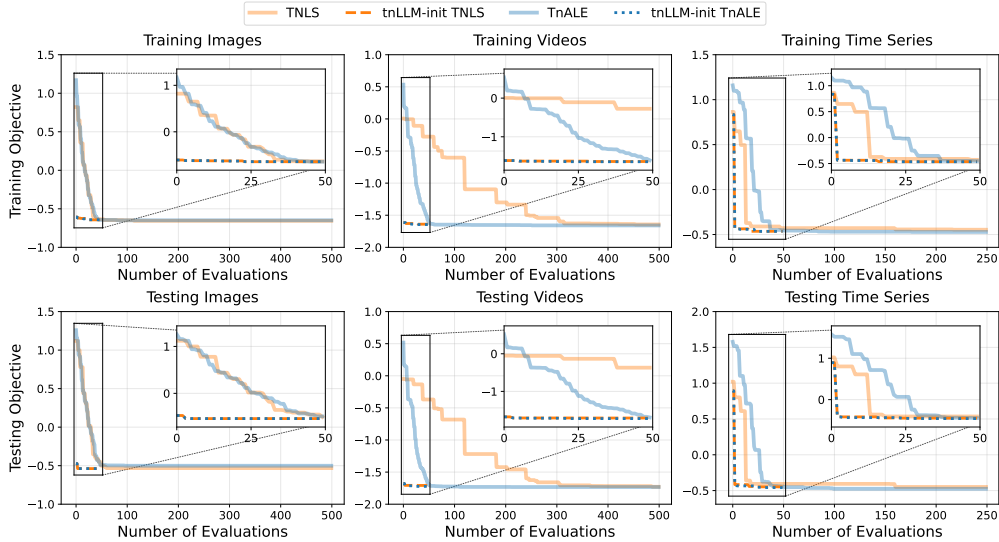


Figure 7: Experimental results across all 3 datasets show that both TNLS and TnALE are significantly accelerated with an initial center of search neighborhood found by tnLLM. We ran TNLS and TnALE with tnLLM initialization in all 3 datasets over 50 evaluations, which *include* the plotted 10 evaluations performed by tnLLM. Vanilla TNLS and TnALE performed 500 evaluations for both the images and videos datasets and 250 evaluations for the financial time-series dataset if not converged.

compared to vanilla TNLS, and up to $13\times$ fewer evaluations compared to vanilla TnALE. The full numerical performance comparison is provided in Appendix G.

4.2 ABLATION STUDY

Removal of domain information. To assess the effectiveness of injecting domain information into the TN-SS problem, we removed the carefully designed structured prompts of the tnLLM framework, equivalent to using the LLM to solve the TN-SS problem without any priors on the domain information. Without domain information, the LLM generates a poorly initialized TN structure that is 80.3% worse in terms of objective function value, due to its lack of information about the different modes, and requires $10.4\times$ more evaluations to converge. Moreover, as the model defaults to random assumptions about the modes, as illustrated in Figure 6, it was found to produce uniformly connected TN structures throughout the minimization process. This restricts the search space to a much smaller set of solutions that are not domain-meaningful from a practical perspective.

Selection of LLM models. To examine how the choice of LLM affects the performance of tnLLM, we compared our baseline model, GPT-4o (gpt-4o-2024-08-06), against GPT-4.5 (gpt-4.5-preview-2025-02-27), GPT4o-mini (gpt-4o-mini-2024-07-18), GPT-3.5 (gpt-3.5-turbo-1106) and the open-source DeepSeek V3 (DeepSeek-V3-0324) model. Observe from Table 2 that due to the carefully designed prompts and the structure of the overall framework, tnLLM is robust to the choice of the LLM used. While there are small variations in the achieved objective function values, the overall performance remained consistent across all three datasets in both training and testing sets. Furthermore, the number of evaluations required by all LLMs falls within the mean \pm standard deviation range reported in Table 1. It is important to note that, despite the consistent performance, weaker models and in particular GPT-3.5 occasionally misinterpreted the optimization objective, mistakenly assuming that higher values were preferable.

5 CONCLUSION

We have introduced tnLLM, a domain-aware LLM-guided TN-SS framework for directly inferring TN structures. This has been achieved by utilizing the rich domain information in real-world tensor

Table 2: Ablation study of using different LLMs within the proposed framework. For different LLMs, we report the best training objective values achieved and their corresponding testing objective values.

Dataset	GPT-4o (Baseline)		GPT-4.5		GPT-4o-mini		GPT-3.5		DeepSeek-V3	
	Train	Test	Train	Test	Train	Test	Train	Test	Train	Test
Images	-0.63	-0.48	-0.62	-0.54	-0.61	-0.48	-0.64	-0.52	-0.62	-0.47
Videos	-1.63	-1.70	-1.62	-1.65	-1.62	-1.69	-1.63	-1.70	-1.63	-1.70
Time-series	-0.42	-0.41	-0.40	-0.41	-0.41	-0.40	-0.42	-0.40	-0.40	-0.39

data and the inherent reasoning capabilities of LLMs. Experimental results have demonstrated that tnLLM achieves performance comparable to current SOTA algorithms, while requiring significantly fewer function evaluations. Notably, by incorporating domain information, our framework is the first to mitigate the black-box nature of the identified TN structures in TN-SS through generating domain-relevant solution explanations. Furthermore, we have shown that tnLLM can be used to accelerate SOTA sampling-based algorithms while preserving their theoretical guarantees.

REFERENCES

- Ziang Chen, Jianfeng Lu, and Anru R. Zhang. One-dimensional tensor network recovery, 2024.
- Kristy Choi, Chris Cundy, Sanjari Srivastava, and Stefano Ermon. LMPriors: Pre-trained language models as task-specific priors. In *NeurIPS 2022 Foundation Models for Decision Making Workshop*, 2022.
- Andrzej Cichocki, Namgil Lee, Ivan Oseledets, Anh Huy Phan, Qibin Zhao, and Danilo P Mandic. Tensor networks for dimensionality reduction and large-scale optimization: Part 1 low-rank tensor decompositions. *Foundations and Trends® in Machine Learning*, 9(4-5):249–429, 2016.
- Tobias Felser, Michele Trenti, Lorenzo Sestini, Alessandro Gianelle, Davide Zuliani, Donatella Lucchesi, and Simone Montangero. Quantum-inspired machine learning on high-energy physics data. *npj Quantum Information*, 7(1):111, 2021.
- Zheng Guo, Aditya Deshpande, Brian Kiedrowski, Xinyu Wang, and Alex Gorodetsky. Tensor network structure search using program synthesis. *arXiv preprint arXiv:2502.02711*, 2025.
- Christopher J. Hillar and Lek-Heng Lim. Most tensor problems are NP-hard. *Journal of the ACM*, 60(6):1–39, 2013.
- Frank L Hitchcock. The expression of a tensor or a polyadic as a sum of products. *Journal of Mathematics and Physics*, 6(1-4):164–189, 1927.
- Takeshi Kojima, Shixiang Shane Gu, Machel Reid, Yutaka Matsuo, and Yusuke Iwasawa. Large language models are zero-shot reasoners. In *Proceedings of the 36th International Conference on Neural Information Processing Systems*, 2024.
- Chao Li and Zhun Sun. Evolutionary topology search for tensor network decomposition. In *Proceedings of the 37th International Conference on Machine Learning*, volume 119 of *Proceedings of Machine Learning Research*, pp. 5947–5957. PMLR, 13–18 Jul 2020.
- Chao Li and Qibin Zhao. Is rank minimization of the essence to learn tensor network structure. In *Second Workshop on Quantum Tensor Networks in Machine Learning (QTNML)*, *Neurips*, volume 3, 2021.
- Chao Li, Junhua Zeng, Zerui Tao, and Qibin Zhao. Permutation search of tensor network structures via local sampling. In *Proceedings of the 39th International Conference on Machine Learning*, pp. 13106–13124, Jul 2022.
- Chao Li, Junhua Zeng, Chunmei Li, Cesar Caiafa, and Qibin Zhao. Alternating local enumeration (TnALE): solving tensor network structure search with fewer evaluations. In *Proceedings of the 40th International Conference on Machine Learning*, ICML’23. JMLR.org, 2023.

- Valentin Liévin, Christoffer Egeberg Hother, Andreas Geert Motzfeldt, and Ole Winther. Can large language models reason about medical questions? *arXiv*, 2023.
- Osman Asif Malik. More efficient sampling for tensor decomposition. *ArXiv*, abs/2110.07631, 2021.
- Eli Meir, Haggai Maron, Shie Mannor, and Gal Chechik. Optimizing tensor network contraction using reinforcement learning. In Kamalika Chaudhuri, Stefanie Jegelka, Le Song, Csaba Szepesvari, Gang Niu, and Sivan Sabato (eds.), *Proceedings of the 39th International Conference on Machine Learning*, pp. 15278–15292. PMLR, 17–23 Jul 2022.
- OpenAI. GPT-4 Technical Report. Technical report, OpenAI, 2023.
- OpenAI. Hello GPT-4o. <https://openai.com/index/hello-gpt-4o/>, 2024.
- Román Orús. A practical introduction to tensor networks: Matrix product states and projected entangled pair states. *Annals of Physics*, 349:117–158, 2014.
- Román Orús. Tensor networks for complex quantum systems. *Nature Reviews Physics*, 1(9):538–550, 2019.
- Ivan V Oseledets. Tensor-train decomposition. *SIAM Journal on Scientific Computing*, 33(5): 2295–2317, 2011.
- Moein Shakeri and Hong Zhang. Moving object detection under discontinuous change in illumination using tensor low-rank and invariant sparse decomposition. In *Proceedings of the IEEE/CVF Conference on Computer Vision and Pattern Recognition (CVPR)*, pp. 7221–7230. IEEE, 2019.
- Karan Singhal, Shekoofeh Azizi, Tinsu Tu, et al. Large language models encode clinical knowledge. *Nature*, 620:172–180, 2023. doi: 10.1038/s41586-023-06291-2.
- Mirac Suzgun, Nathan Scales, Nathanael Schärli, Sebastian Gehrmann, Yi Tay, Hyung Won Chung, Aakanksha Chowdhery, Quoc Le, Ed Chi, Denny Zhou, and Jason Wei. Challenging BIG-bench tasks and whether chain-of-thought can solve them. In *Findings of the Association for Computational Linguistics: ACL 2023*. Association for Computational Linguistics, July 2023.
- Hugo Touvron, Thibaut Lavril, Gautier Izacard, Xavier Martinet, Marie-Anne Lachaux, Timothée Lacroix, Baptiste Rozière, Naman Goyal, Eric Hambro, Faisal Azhar, et al. Llama: Open and efficient foundation language models. *arXiv preprint arXiv:2302.13971*, 2023.
- Ledyard R Tucker. Some mathematical notes on three-mode factor analysis. *Psychometrika*, 31(3): 279–311, 1966.
- Jason Wei, Yi Tay, Rishi Bommasani, Colin Raffel, Barret Zoph, Sebastian Borgeaud, Dani Yogatama, Maarten Bosma, Denny Zhou, Donald Metzler, Ed H. Chi, Tatsunori Hashimoto, Oriol Vinyals, Percy Liang, Jeff Dean, and William Fedus. Emergent abilities of large language models. *Transactions on Machine Learning Research*, 2022a. ISSN 2835-8856.
- Jason Wei, Xuezhi Wang, Dale Schuurmans, Maarten Bosma, brian ichter, Fei Xia, Ed H. Chi, Quoc V Le, and Denny Zhou. Chain of thought prompting elicits reasoning in large language models. In *Advances in Neural Information Processing Systems*, 2022b.
- Zhong-Cheng Wu, Ting-Zhu Huang, Liang-Jian Deng, Hong-Xia Dou, and Deyu Meng. Tensor wheel decomposition and its tensor completion application. *Advances in Neural Information Processing Systems*, 35:27008–27020, 2022.
- Ryuki Yamamoto, Hidekata Hontani, Akira Imakura, and Tatsuya Yokota. Fast algorithm for low-rank tensor completion in delay-embedded space. In *Proceedings of the IEEE/CVF Conference on Computer Vision and Pattern Recognition (CVPR)*, pp. 2048–2056. IEEE, 2022.
- Ke Ye and Lek-Heng Lim. Tensor network ranks. *arXiv preprint arXiv:1801.02662*, 2018.
- Tatsuya Yokota, Burak Erem, Seyhmus Guler, Simon K Warfield, and Hidekata Hontani. Missing slice recovery for tensors using a low-rank model in embedded space. In *Proceedings of the IEEE Conference on Computer Vision and Pattern Recognition*, pp. 8251–8259, 2018.

- Junhua Zeng, Chao Li, Zhun Sun, Qibin Zhao, and Guoxu Zhou. tnGPS: Discovering unknown tensor network structure search algorithms via large language models (LLMs). In *Proceedings of the Forty-first International Conference on Machine Learning*, 2024a.
- Junhua Zeng, Guoxu Zhou, Yuning Qiu, Chao Li, and Qibin Zhao. Bayesian tensor network structure search and its application to tensor completion. *Neural Networks*, 175(C), July 2024b.
- Qibin Zhao, Guoxu Zhou, Shengli Xie, Liqing Zhang, and Andrzej Cichocki. Tensor ring decomposition. *arXiv preprint arXiv:1606.05535*, 2016.
- Shandian Zhe, Zenglin Xu, Xinqi Chu, Yuan Qi, and Youngja Park. Scalable nonparametric multiway data analysis. In *Proceedings of the Eighteenth International Conference on Artificial Intelligence and Statistics*, pp. 1125–1134. PMLR, 2015.
- Wen-Jie Zheng, Xi-Le Zhao, Yu-Bang Zheng, Jie Lin, Lina Zhuang, and Ting-Zhu Huang. Spatial-spectral-temporal connective tensor network decomposition for thick cloud removal. *ISPRS Journal of Photogrammetry and Remote Sensing*, 199:182–194, 2023.
- Yu-Bang Zheng, Ting-Zhu Huang, Xi-Le Zhao, Qibin Zhao, and Tai-Xiang Jiang. Fully-connected tensor network decomposition and its application to higher-order tensor completion. *Proceedings of the AAAI Conference on Artificial Intelligence*, 35(12):11071–11078, May 2021.
- Yu-Bang Zheng, Xi-Le Zhao, Junhua Zeng, Chao Li, Qibin Zhao, Heng-Chao Li, and Ting-Zhu Huang. SVDinsTN: A tensor network paradigm for efficient structure search from regularized modeling perspective. In *Proceedings of the IEEE/CVF Conference on Computer Vision and Pattern Recognition*, 2024.

A LIMITATIONS AND FUTURE WORK

Despite the good performance, the proposed domain-aware TN-SS framework currently lacks theoretical guarantees for its evaluation efficiency due to the black-box nature of LLMs. This could be mitigated by developing domain-aware TN-SS algorithms based on continuous optimization. Also, as mentioned in the ablation study, weaker LLM models, such as GPT-3.5, were found to be more prone to misinterpret the optimization objectives. Therefore, improving the reasoning consistency of smaller LLM models promises to further improve the efficiency of the framework. Furthermore, prompt learning is an active area of research in LLMs, which can be used to potentially enhance the tnLLM framework in future works.

B FULL PROMPTS OF TNLLM FRAMEWORK

The full “Behavior-directive”, “Task-directive” and “Optimization-directive” prompts used in the tnLLM framework are illustrated in Figures 8, 9, 10, respectively.

"" You are a <domain> expert specialized in tensor decomposition. Your task is to <task description>. You need to provide <solution description> which minimizes the loss function, which is the natural log of the sum of the compression rate and 10 times the approximation error. The compression ratio is calculated as the number of parameters in the compressed FCTND format divided by the original number of parameters of the uncompressed tensor and the approximation error is the relative square error between the original and approximate tensor. Work your suggestions out step-by-step based on rigorous reasoning and <domain> knowledge. Explain your final suggestions in a logical, concise manner.""

Figure 8: The full “Behavior-directive” prompt.

""We are working with a fully connected <tensor size> tensor representing <domain> data with the following modes: <Description of each mode including its size and content>

Your task is to suggest the optimal solution for each connection in a fully connected tensor network decomposition. The loss function to minimize is a natural log of the sum of the compression rate and 10 times the tensor approximation error which is the relative square error between the original and approximate tensor. Provide your response in the following format:

1. Take a deep breath and reason step-by-step about the intrinsic interactions between every pair of modes based on your understanding of the relationships about <mode information>. It is important to reason about those intrinsic interactions based on interpretable factors.
2. Based on your reasoning, output <solution description>.

Output format:
Reasoning: Reason about the intrinsic interactions between every pair of modes based on your understanding of <domain> data.

Solution: <Exact solution format>
End the output message with <description of solution format>.""

Figure 9: The full “Task-directive” prompt.

C DATA

We constructed a custom financial time series dataset with 142 temporally ordered fifth-order tensors, denoted as $\{\mathcal{X}_n\}_{n=1}^{142} \in \mathbb{R}^{3 \times 6 \times 3 \times 4 \times 5}$, each representing a rolling window produced via multi-way delay embedding through the temporal direction (Yokota et al., 2018). This leads to the value selection process of 10 ranks. To the best of our knowledge, this is the largest tensor dataset in terms of number of samples ever considered in the TN-SS problem. The first 80% of these tensors were used as the training data, while the remaining 20% with non-overlapping entries with the training data were used for testing. The modes of each time series tensor correspond to:

- **Mode 1:** Types of financial instruments. They are equity indices, commodities, and currency swaps.

"" The last solution is <last_solution> with a total loss function of <last_loss>, which is the natural log of the sum of the current compression rate of <last_compression_rate> and 10 times the current approximation error of <last_approximation_error>. The lowest total loss function is <best_objective_function> which is the natural log of the sum of the compression rate of <best_compression_rate> and ten times the approximation error of <best_approximation_error> is found by using the solution <best_solution>. The loss function to minimize is a natural log of the sum of the compression rate and 10 times the tensor approximation error which is the relative square error between the original and approximate tensor.

Take a deep breath, refine the solution suggestions to make the loss function smaller, and justify any changes in the solution. Keep in mind that increasing the ranks significantly decreases the approximation error, while it increases the compression rate. However, if the compression rate is already very low compared to the approximation error (for example, the compression rate is smaller than half of the approximation error), increasing the ranks (such as doubling it) to decrease the approximation error will usually lead to a lower loss function. Also, if the compression rate is already very high compared to the approximation error (for example, the compression rate is larger than two times the approximation error), reducing the ranks (such as cutting it in half) to decrease the compression rate will usually lead to a lower loss function.

When refining the ranks, consider how each mode <mode titles> interacts with the others and how reducing or increasing the rank will affect the overall decomposition accuracy. You are encouraged to be explorative to try small and large rank value changes in this process. Do not change ranks if you think its not necessary. You should never try the same set of ranks more than once. Trying the same set of ranks more than once wastes computation resources and will not lead to a different outcome.

Provide the solution and reason step-by-step for the changes in the following format:
Output format:
Reasoning: Reason about the intrinsic interactions between every pair of modes based on your understanding of <domain> data.
Solution: <Exact solution format>
End the output message with <description of solution format>. ""

Figure 10: The full ‘‘Optimization-directive’’ prompt.

- **Mode 2:** Assets within each type of financial instrument. For equity indices, these are Hang Seng, Nikkei 225, S&P 500, EURO STOXX 50, FTSE 100, and Shanghai Composite Index. For commodities, these are Brent Crude, Copper, Natural gas, Comex gold, Soybeans, and Wheat. For currency swaps, these are HKD/USD, JPY/USD, CHF/USD, EUR/USD, CNY/USD, and GBP/USD.
- **Mode 3:** Features of each asset. These are average adjusted closing price log return, average relative price min-max, and average high-low spread.
- **Mode 4:** Interval of time points on which we calculate the average features. There are 4 intervals – 1 day, 5 days, 10 days, and 15 days.
- **Mode 5:** Time points within each rolling window of length 5.

The images and videos datasets are fetched from <http://trace.eas.asu.edu/yuv/>. Figure 11 illustrates 5 example image samples, $\{\mathcal{X}_n\}_{n=1}^5 \in \mathbb{R}^{144 \times 176 \times 3}$, used in the experiments. The first 80% of these tensors were used as the training data, while the remaining 20% for testing. The modes of each image tensor correspond to:

- **Mode 1:** Height of the image. These are the vertical pixel indexes.
- **Mode 2:** Width of the image. These are the horizontal pixel indexes.
- **Mode 3:** RGB channels. These are the red, green, and blue channels.



Figure 11: Image samples used in the experiments.

Video dataset is produced from performing the multi-way delay embedding (Yamamoto et al., 2022) through the temporal mode in a video to produce 5 samples, $\{\mathcal{X}_n\}_{n=1}^5 \in \mathbb{R}^{144 \times 176 \times 3 \times 10}$. Figure 12

shows an example sample of the videos dataset at different frames. The modes of each video tensor correspond to:

- **Mode 1:** Height of the image. These are the vertical pixel indexes.
- **Mode 2:** Width of the image. These are the horizontal pixel indexes.
- **Mode 3:** RGB channels. These are the red, green, and blue channels.
- **Mode 4:** Frames in a video. These are the index of the frames in a video.

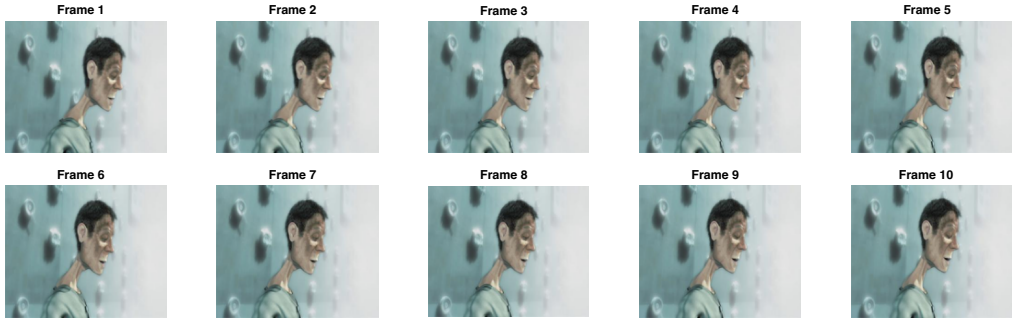


Figure 12: One example sample of the Video data used in the experiments.

D IMPLEMENTATION DETAILS

All baseline models are initialized as a “fully-disconnected” graph. The TN search template is set to a complete graph. For TNLS, we set the number of samples (evaluations), $\#Sample$, in each sampling step to 4 in the images dataset, 60 in the videos dataset, and 10 in the time series dataset. For TnALE, we set $D = 1$, $r = 1$. For tnGPS, we selected the best-performing algorithm discovered (“Ho-2”) and adopted the following hyperparameters as suggested in their paper: code upper bound of 10, mutation rate of 0.1, crossover rate of 0.6, selection pressure of 1.5, elitism enabled, diversity factor of 0.05, variance decay of 0.98, minimum variance of 0.1, tournament size factor of 0.2, elite diversity boost of 2.0, random individual chance of 0.05, and a maximum mutation of 3. All models were run for 500 evaluations in both the images and videos dataset, and 250 evaluations in the time series dataset if not converged. An internal server with NVIDIA RTX A6000 GPU, an AMD Ryzen Threadripper PRO 5955WX with 16 cores, and 256GB of RAM was used.

E RUNTIME COMPARISONS

Table 3 reports the total average runtime in seconds to first achieve the best training objective function value for all models across the three datasets of Table 1. For tnLLM, this also includes the LLM inference time. The proposed tnLLM achieves comparable performance to SOTA methods while reducing runtime by up to 98.3% compared to TNLS, 97.7% compared to TnALE, and 98.1% compared to tnGPS.

Table 3: Runtime comparisons across three datasets. The values are the total average runtime in seconds to first achieve the best training objective function value. A lower value is better. The best values are denoted in bold. The second best values are underlined.

Data Type	TNLS	TnALE	tnGPS	tnLLM (Ours)
Images	2,122s	<u>1,659s</u>	8,025s	151s
Videos	17,690s	<u>15,298s</u>	20,461s	1,984s
Time-series	110,945s	<u>80,700s</u>	<u>17,287s</u>	1,866s

F SUMMARIZED GENERATED EXPLANATIONS OF TNLLM FOR THE INITIALIZED TN STRUCTURE

The full set of summarized LLM generated explanations over three independent runs for the images, videos, and time-series datasets are provided in Tables 4, 5, and 6, respectively. The suggested ranks are verified to be consistent with the domain-informed reasoning provided by tnLLM. Also, the domain-relevant explanations are robust across multiple runs.

Table 4: Summarized generated explanations of tnLLM for the initialized TN structure in the Images dataset over 3 independent runs.

Mode Pair	Run 1	Run 2	Run 3
Mode 1 & Mode 2 (Width ↔ Height)	<ul style="list-style-type: none"> • Defines spatial resolution • Spatial coherence is significant due to smoothness • High rank needed to capture spatial detail (suggested rank: 20) 	<ul style="list-style-type: none"> • Spatial dimensions are highly correlated • Captures patterns and structures • High rank to capture spatial complexity (suggested rank: 20) 	<ul style="list-style-type: none"> • Spatial resolution key for details and patterns • High rank crucial to capture more spatial features to maintain image quality • High rank (suggested rank: 20)
Mode 1 & Mode 3 (Width ↔ RGB)	<ul style="list-style-type: none"> • Captures horizontal color distribution • Less complex than spatial features • Moderate rank to capture color variation without overfitting (suggested rank: 5) 	<ul style="list-style-type: none"> • Horizontal color changes are smooth • Color variations less complex as object maintains consistent color across width • Moderate rank (suggested rank: 5) 	<ul style="list-style-type: none"> • Related through color distribution along width • Color variations less complex than spatial variation • Moderate rank (suggested rank: 5)
Mode 2 & Mode 3 (Height ↔ RGB)	<ul style="list-style-type: none"> • Captures vertical color patterns • Vertical and horizontal color distributions often equally important • Rank should be similar to the width-RGB connection (suggested rank: 5) 	<ul style="list-style-type: none"> • Captures vertical color variation • Vertical structures (e.g., stripes) may add complexity • Rank might be slightly higher than width-channel rank (suggested rank: 8) 	<ul style="list-style-type: none"> • Complexity of color variation along height and width typically similar • Moderate rank is also appropriate (suggested rank: 5)

G PERFORMANCE COMPARISON FOR VANILLA AND TNLLM-INITIALIZED TNLS AND TNALE

Table 7 illustrates the detailed performance of vanilla and tnLLM-initialized TNLS and TnALE across different datasets.

Table 5: Summarized generated explanations of tnLLM for the initialized TN structure in the Videos dataset over 3 independent runs.

Mode Pair	Run 1	Run 2	Run 3
Mode 1 & Mode 2 (Width ↔ Height)	<ul style="list-style-type: none"> • Defines spatial resolution per frame • Needs to capture spatial detail for video quality but balance with compression • Moderate-to-high rank (suggested rank: 20) 	<ul style="list-style-type: none"> • Define spatial resolution per frame • Higher rank captures more complex spatial patterns and correlations • Moderate-to-high rank to balance detail capture and compression (suggested rank: 20) 	<ul style="list-style-type: none"> • Define spatial resolution per frame • Spatial resolution is a significant aspect of video quality • Moderate-to-high rank to capture more spatial details across frames (suggested rank: 20)
Mode 1 & Mode 3, Mode 2 & Mode 3 (Width/Height ↔ RGB)	<ul style="list-style-type: none"> • Less complex than spatial info • Limited variation of color across width/height • Low rank suffices (suggested rank: 5) 	<ul style="list-style-type: none"> • Less directly correlated than spatial dimensions • Certain horizontal/vertical patterns prominent in specific color channels • Low rank suffices (suggested rank: 5) 	<ul style="list-style-type: none"> • Captures color variations horizontally/vertically • Color variations can be significant in videos with rich color content • Moderate-to-low rank (suggested rank: 5)
Mode 1 & Mode 4, Mode 2 & Mode 4 (Width/Height ↔ Frames)	<ul style="list-style-type: none"> • Captures horizontal/vertical structure changes over time • Videos have temporal consistency • Moderate rank (suggested rank: 10) 	<ul style="list-style-type: none"> • Related through motion and changes across frames • Moderate rank to capture temporal changes across width/height of the video (suggested rank: 10) 	<ul style="list-style-type: none"> • Captures temporal variations across the horizontal/vertical dimension • Temporal changes crucial for motion representation • Moderate rank (suggested rank: 10)
Mode 3 & Mode 4 (RGB ↔ Frames)	<ul style="list-style-type: none"> • Captures color changes over time • Color changes often subtle and less complex than spatial changes • Lower rank can be used to maintain compression (suggested rank: 3) 	<ul style="list-style-type: none"> • Captures color changes over time • Crucial for capturing dynamic color variations and transitions • Low rank to model temporal color variation (suggested rank: 5) 	<ul style="list-style-type: none"> • Captures temporal color changes • Essential for representing dynamic scenes • Moderate-to-low rank necessary to capture these changes (suggested rank: 5)

Table 6: Summarized generated explanations of tnLLM for the initialized TN structure in the Time-series dataset over 3 independent runs.

Mode Pair	Run 1	Run 2	Run 3
Mode 1 & Mode 2 (Types of financial instruments ↔ Assets within each type)	<ul style="list-style-type: none"> • Strong intrinsic relationship • Different assets within a type exhibit correlated behaviors due to shared market factors • Higher rank (suggested rank: 3) 	<ul style="list-style-type: none"> • Strong relationship as each type is defined by its constituent assets • High diversity and specificity across assets • Higher rank (suggested rank: 3) 	<ul style="list-style-type: none"> • Strong connection as each instrument has specific assets • Rank should reflect the diversity and specificity of assets within each type • Higher rank (suggested rank: 3)
Mode 1 & Mode 3 (Types of financial instruments ↔ Features of each asset)	<ul style="list-style-type: none"> • Features influenced by instrument type • For example, volatility of commodities might differ from that of equity indexes • Moderate rank (suggested rank: 2) 	<ul style="list-style-type: none"> • Different instruments behave distinctly (returns, volatility, spreads) • Features somewhat standardized across types • Moderate rank to not overfit (suggested rank: 2) 	<ul style="list-style-type: none"> • Instruments behave differently in terms of features • However, features themselves are common across all types • Moderate rank to capture variability (suggested rank: 2)
Mode 2 & Mode 3 (Assets within each type ↔ Features of each asset)	<ul style="list-style-type: none"> • Features directly derived from assets indicating strong relationship • Different assets have distinct feature profiles • Higher rank (suggested rank: 3) 	<ul style="list-style-type: none"> • Each asset has unique characteristics in terms of returns, volatility, and spreads • Higher rank to accurately capture specific features (suggested rank: 3) 	<ul style="list-style-type: none"> • Each asset has unique characteristics in terms of features like log returns and spreads • Higher rank needed for this detailed interaction (suggested rank: 3)
Mode 4 & Mode 5 (Interval of time points ↔ Time points in each rolling window)	<ul style="list-style-type: none"> • Inherently linked as rolling window defines the context for the time points • Moderate rank (suggested rank: 2) 	<ul style="list-style-type: none"> • Weak relationship as rolling window smooths out short-term variations • Lower rank is suitable (suggested rank: 1) 	<ul style="list-style-type: none"> • Intrinsic connection as time points are nested within the intervals • Moderate rank to capture this structure (suggested rank: 2)

Table 7: Performance comparison across different datasets for vanilla and tnLLM-initialized TNLS and TnALE. The values on the left give the lowest training objective function values and their corresponding testing objective function values. The values in [square brackets] give the number of evaluations required to first achieve the best training objective function value. For both metrics, a lower value is better. The least number of evaluations are highlighted in bold.

Data Type		TNLS				TnALE			
		Vanilla		tnLLM-init		Vanilla		tnLLM-init	
Images	Train	-0.66	[114]	-0.64	[20]	-0.65	[81]	-0.64	[19]
	Test	-0.47		-0.46		-0.46		-0.46	
Videos	Train	-1.64	[484]	-1.64	[21]	-1.66	[254]	-1.65	[20]
	Test	-1.72		-1.71		-1.72		-1.70	
Time-series	Train	-0.45	[218]	-0.47	[14]	-0.47	[177]	-0.47	[20]
	Test	-0.43		-0.44		-0.47		-0.44	